USGS Toxic Substances Hydrology Program–Proceedings of the Technical Meeting, Charleston, S.C., March 8–12, 1999, Morganwalp, D.W., and Buxton, H.T. (editors), USGS Water-Resources Investigations Report 99-4018C, Vol. 3 of 3, Subsurface Contamination from Point Sources, p. 821-832.

Modifications to the Solute-Transport Model MOC3D for Simple Reactions, Double Porosity, and Age, with Application at Mirror Lake, New Hampshire, and Other Sites

By Daniel J. Goode

ABSTRACT

The U.S. Geological Survey (USGS) three-dimensional solute-transport model MOC3D has been extended to increase the flexibility of first- and zero-order reaction terms to approximate geochemical reactions and to simulate double-porosity exchange and ground-water age. The flexibility of first- and zero-order reaction modeling is increased by allowing the rate coefficients to vary from cell to cell in space and to change in time in a step-wise manner. This flexibility improves the ability of this single-solute model to approximate the effects of multi-species solute interactions during reactive transport. Double-porosity exchange accounts for diffusive exchange of solute mass between water flowing in the aquifer and immobile water. This first-order formulation can approximate the effects of dead-end pores or matrix diffusion. Ground-water age is simulated by a zero-order source term of unit strength that accounts for the aging of water during transport. Using this option, the output from the model is the spatial distribution of age and the volume-weighted age of mixtures such as water in discharging wells. These new capabilities are illustrated by applications at Mirror Lake, N.H., and at other sites where research on transport in ground water has been carried out through the USGS Toxic Substances Hydrology Program.

CAPABILITIES OF MOC3D

This paper summarizes the existing and new capabilities of the U.S. Geological Survey (USGS) three-dimensional solute-transport model MOC3D (Konikow and others, 1996). Full documentation of the modifications described here (in review), are expected to be made available in 1999 on the web at <http://water.usgs.gov/software/moc3d.html>.

Solute-Transport Simulation

MOC3D is a general-purpose computer model developed by the USGS for simulation of three-dimensional solute transport in ground water (Konikow and others, 1996). The model is an update to the widely used USGS two-dimensional solute-transport model (MOC) and is implemented as an optional 'package' for the ground-water flow model MODFLOW (Harbaugh and McDonald, 1996). The model simulates transport processes affecting a single solute in saturated ground water that include:

- Advection - Transport of a dissolved solute at the same rate as the average ground-water flow velocity.
- Diffusion - Spreading of solute from areas of high concentration to areas of low concentration, caused by 'random' molecular motion.
- Dispersion - Diffusion-like spreading of solute that is caused primarily by spatial variability in aquifer properties, which in turn causes spatial variability in transport velocity.
- Retardation^{+} - Reduction in the apparent solute velocity, compared to the ground-water velocity, caused by linear equilibrium sorption on aquifer materials.
- Decay^{+} - Disappearance of solute caused by reactions such as radioactive decay or biodegradation that are proportional to concentration.
- Growth* - Creation (or disppearance) of solute mass caused by reactions that proceed independent of the solute concentration, such as some biodegradation processes.
- Double-porosity exchange* - rate-limited exchange of solute mass between mobile

and immobile phases, for example between fractures and rock matrix.

The symbol * indicates new model capabilities. The symbol $^{+}$ indicates model capabilities that have increased flexibility with the modifications discussed here. MOC3D also accounts for solute sources and sinks associated with a wide range of water sources and sinks.

Growth is a zero-order internal source of solute specified as a mass rate per unit volume of water. This reaction is independent of solute concentration. If the growth rate is specified as negative, this is the rate of loss of solute mass. In this case, the reaction rate changes to zero when the concentration decreases to zero. The growth rate is allowed to vary spatially from cell to cell in the model and to change in time. Sorbed solute may have a separate growth rate.

Double-porosity exchange is a simple model of the diffusive exchange of solute mass between flowing water in the aquifer and immobile or nearly immobile water. Applications include simulation of dead-end pores or porosity within solid grains in granular porous media and matrix diffusion in fractured rock. The mass exchange rate is given by the product of a linear exchange coefficient and the concentration difference between the flowing water and water in the immobile phase. Within the immobile phase, zero-order growth and first-order decay can be simulated.

The retardation factor, which originally could be changed layer by layer, is now allowed to vary spatially from cell to cell in the model. Likewise, the decay rate coefficient, which originally was uniform throughout the model, is now allowed to vary spatially from cell to cell in the model. Furthermore, sorbed solute can decay at a different rate than dissolved solute, and the decay rate can change in time.

Simulation of Ground-Water Age

The volume-weighted average age of ground water in an aquifer may be simulated by use of a standard solute-transport equation with an additional zero-order source term of unit strength (Goode, 1996, 1998). The output from the model is the age, or time since the water entered the aquifer, at all locations. Furthermore, the volumetric average age of a mixed discharge, such as that at a pumping well, is computed. Boundary and initial conditions for the transport equation are similar to the solute transport case. Generally, incoming water is assumed to have age zero, by definition. External sources of ground water, however, such as an adjacent aquifer, can be simulated as water sources with specified age. Most model applications will probably be for steady-state age, in which case the initial condition is not needed, mathematically. Transient age simulations require that the initial age throughout the aquifer be specified.

The primary advantage of this method over particle tracking for modeling ground-water age is that the effects of diffusion, dispersion, and other mixing processes are directly handled through the solute-transport equation. In cases where dispersion is low, results of this method should generally agree with particle tracking. The effect of longitudinal dispersion is limited because age gradients along a streamline are by definition gradual, hence the 'age flux' due to these gradients is also small. Steep age gradients can exist in the direction perpendicular to flow, however, and the resulting transverse diffusion or dispersion can have significant effects on ground-water age (Goode, 1996).

EXAMPLES OF MOC3D CAPABILITIES

The following examples illustrate some of the capabilities of MOC3D for simulation of spatially variable reactions and ground-water age. Comparison of simulation results to analytical solutions for simple test cases, which are not presented here, demonstrate that the numerical methods used can accurately solve the governing equations under restrictive test conditions. The examples here serve to illustrate the use of MOC3D as a general-purpose hydrogeologic tool.

Approximation of Biodegradation Using Spatially Variable Decay Rates

An illustrative simulation uses time- and space-varying decay coefficients to approximate biodegradation of benzene at the Laurel Bay, S.C., research site (Landmeyer and others, 1998). Benzene attenuation depends on decay rates that are generally higher in aerobic (oxygen rich) zones and lower in anaerobic (zero oxygen) zones (fig. 1). In fact, anaerobic biodegradation rates are dependent on the specific terminal-electron-accepting-process (TEAP) controlling the redox state.

The estimated first-order biodegradation decay rates for benzene at Laurel Bay vary from 0.0005 to 0.1 /day (per day), depending on the redox conditions. Fast aerobic degradation takes place outside the anaerobic zones, except at early time when the microbes are assumed to be in low concentrations. As oxygen is consumed, the area of anaerobic redox conditions spreads. Degradation rates are lower in the iron and sulfate reduction zones than in the aerobic zone and are lowest in the methanogenic (carbon dioxide) TEAP zone in the center of the plume.

MOC3D simulation with temporally and spatially varying decay coefficients realistically approximates the extent of benzene migration observed at the site, which can not be modeled successfully by use of a single decay coefficient. A transect through the center of the simulated plume, transverse to the general direction of flow is shown in figure 1. The shaded area indicates the area of iron and sulfate reduction that is modeled using a decay rate of 0.001 /day. In the center of the plume, methanogenesis is occurring, which is modeled using a decay rate of 0.0005 /day. At the time of the illustration, aerobic degradation rates are very high, 0.1 /day. The flexibility to vary the decay rate from cell to cell allows the simulation to capture the rapid degradation of benzene on the outskirts of the plume as well as the elevated concentrations in the center of the plume, where degradation is slow. The simulation with a uniform decay rate of 0.001 /day overestimates benzene concentrations in the aerobic zone and underestimates concentrations in the plume center.

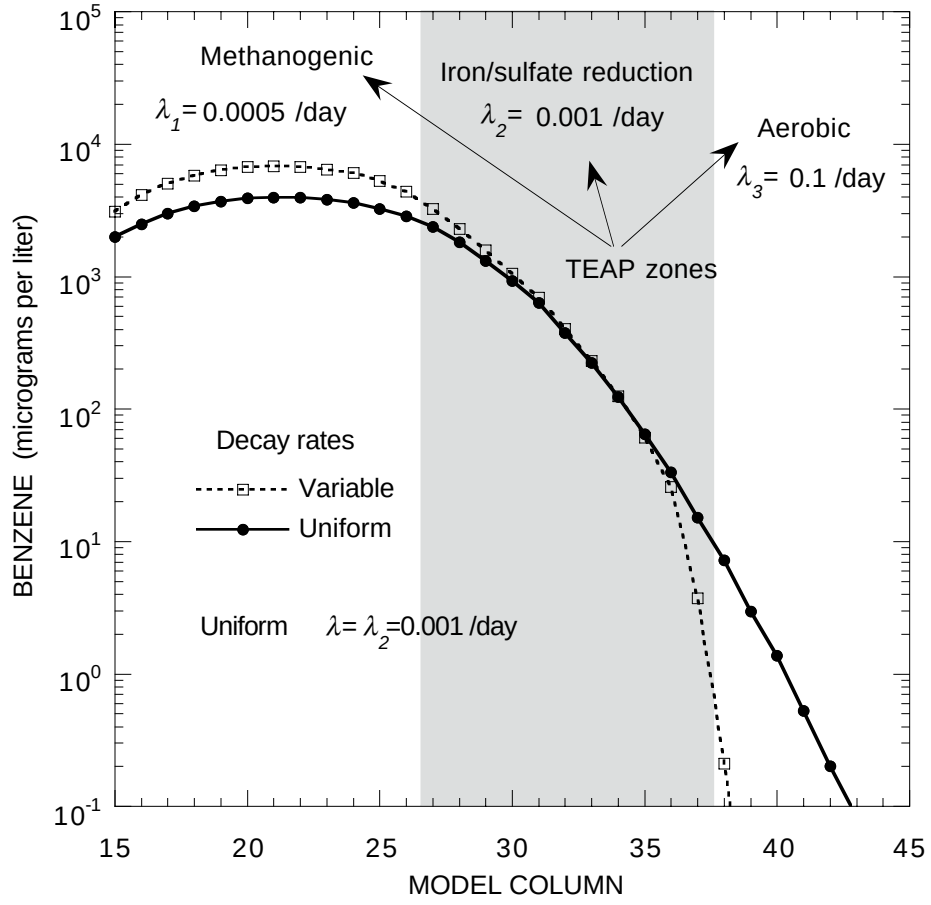

Figure 1. Comparison of benzene concentrations along a transverse transect spanning three terminal-electron-accepting-process (TEAP) zones simulated by use of MOC3D with spatially variable decay rates *(λ_1, λ_2, λ_3)* to concentrations simulated with a uniform decay rate *(λ)*.

Two-Dimensional Age Distribution in a Mildly Heterogeneous Aquifer

Simulation of the age distribution in a hypothetical aquifer illustrates features of ground-water age in mildly heterogeneous porous media. Intensive field tracer experiments have been conducted at a military reservation on Cape Cod, Mass. LeBlanc and others (1991) describe a natural gradient tracer test conducted over 2 years using nonreactive and reactive tracers in a mildly heterogeneous sand and gravel aquifer. Garabedian and others (1991) analyze the spreading of a nonreactive tracer and estimate asymptotic dispersivities from the temporal growth in the spatial moments of the tracer distribution. Hess and others (1992) compare field and laboratory measurements of hydraulic conductivity and estimate macrodispersivities from theoretical relations.

A hypothetical two-dimensional aquifer is generated that has heterogeneous hydraulic conductivity with spatial statistics similar to those from the Cape Cod tracer test. The turning bands method (Mantoglou and Wilson, 1982; Zimmerman and Wilson, 1989) is used to generate a spatially correlated field of hydraulic conductivity *(K)*. Hydraulic conductivity is assumed to be lognormally distributed with mean 110 m/d (meters per day) (Garabedian and others, 1991) and variance of the natural log of K = 0.24 (Hess and others, 1992). An exponential spatial covariance function is assumed with zero nugget and isotropic correlation length of 2.6 m (meters) (Hess and others, 1992). The grid is 100 m by 20 m and is discretized by 500 x 100 square blocks having $\Delta x = \Delta y$ = 0.2 m. The single realization of K used (fig. 2) reflects the underlying statistical properties: most of the K values are clustered near and below the mean, the size of the high and low zones are larger than individual grid blocks and smaller than the grid dimensions, and only a few isolated zones exhibit K > 300 m/d.

The boundary conditions for the steady-state flow model are fixed hydraulic head $h(x = 0)$ = 0.148 m; $h(x$ = 100 m) = 0 m; and no-flow at y = 0 and y = 20 m. These boundary conditions, along with an assumed porosity of 0.39 (LeBlanc and others, 1991), yield an average velocity of about 0.4 m/d.

The steady-state age distribution (fig. 2b) is more variable than the head distribution and indicates significant persistence of thin 'fingers' of contrasting age. Youngest ages are along a somewhat continuous zone of elevated K in the upper half (y < 10 m) of the aquifer. An adjacent zone with older water, however, reflects the effect of a large zone of low K located at about (x,y) = (20 m, 5 m). The resulting large difference in age between closely spaced streamlines persists downstream to the end of the aquifer. The variable traveltimes of different streamlines would be modeled as longitudinal dispersion if the small-scale K variability were not explicitly simulated.

The spatial variability of the steady-state age distribution can also be illustrated by plots of age as a function of distance. In the longitudinal direction, the age generally increases more or less smoothly in the average direction of flow (fig. 3). For much of the domain, the variability in the x-direction is relatively smooth, as illustrated by the transects at y = 7.3 and 13.3 m. The overall rate of increase in age versus x shown for these two transects essentially brackets all longitudinal transects in this simulation. Significantly more variability along x is illustrated near the position of the large low-K zone, as shown by the transect at y = 5.3 m. At this position, the age does not monotonically increase in the mean direction of flow. For example, the water at (x, y) = (45 m, 5.3 m) is about 30 days older than water 5 m further down (the mean) gradient at (x,y) = (50 m, 5.3 m). Close examination of other transects indicates that in this simulation all transects have portions where age decreases in the mean flow direction. This decrease in age in the mean flow direction is due to the difference between the actual streamlines and the mean path.

Variability in age is pronounced in the y-direction, transverse to the mean flow direction (fig. 4). The variability is less at the upstream boundary because by definition the age is uniform at 0 days at x = 0. A significant peak of older water develops between x = 10 and 30 m because of the large low-K zone discussed above. Although the y position of this peak shifts due to shifting streamlines, the magnitude of the difference between the age on this peak and on adjacent streamlines persists through the simulated domain.

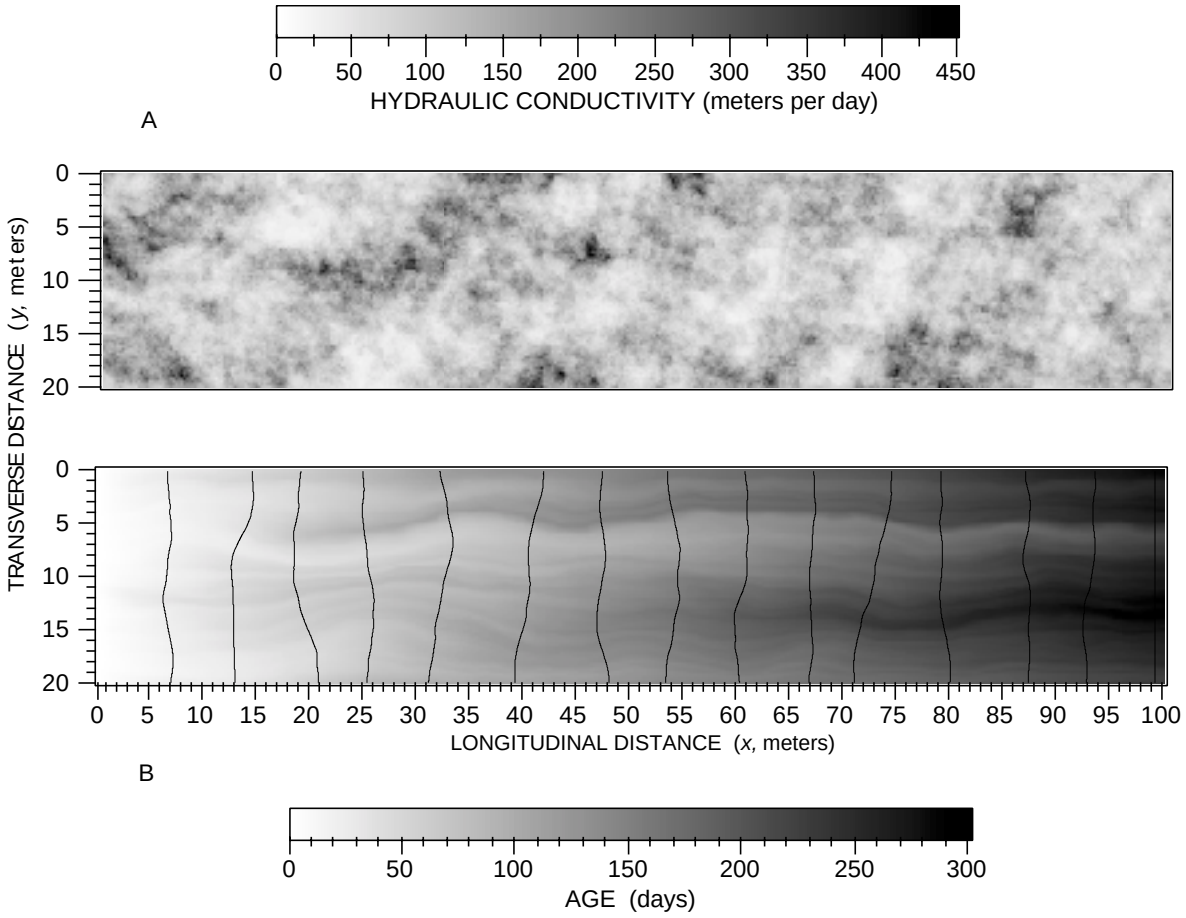

Figure 2. Age simulation in a mildly heterogeneous two-dimensional aquifer: (a) Hydraulic conductivity distribution; (b) Hydraulic head contours (0.01 m interval) and age distribution for advection-only.

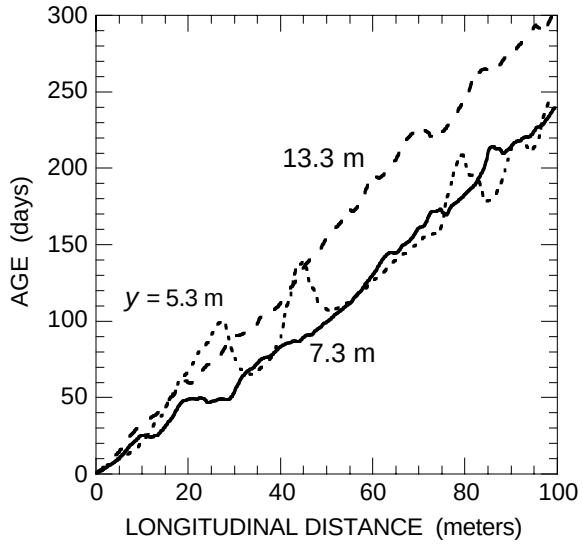

Figure 3. Age variation along transects oriented longitudinal to the average flow direction for a mildly heterogeneous two-dimensional aquifer. The transverse location of each transect is given by *y.*

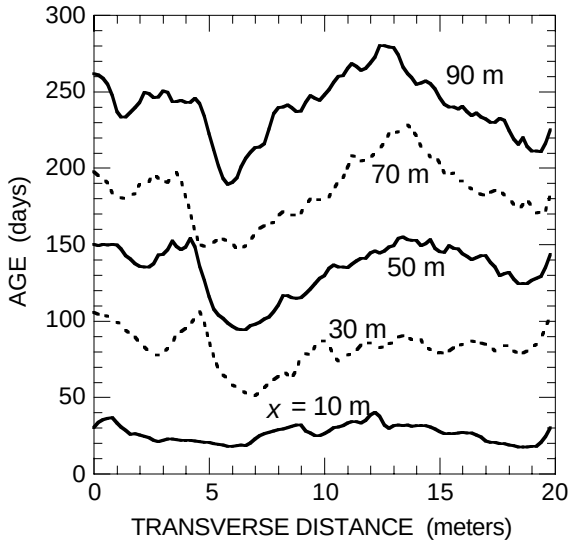

Figure 4. Age variation along transects oriented transverse to the average flow direction for a mildly heterogeneous two-dimensional aquifer. The longitudinal location of each transect is given by *x.*

Age of Samples Pumped from a Heterogeneous Formation

The age of the water in a ground-water system can be estimated from concentrations of environmental tracers in samples pumped from wells. For example, the time since water has been isolated from the atmosphere can be estimated from concentrations of chlorofluorocarbons (CFC's) because atmospheric concentrations have been increasing for about the last 50 years (Plummer and others, 1993). When drawing water from a well, particularly one with a long screened or open interval, the pumped water is a mixture of water from different parts of the aquifer. This mixing can significantly complicate or add uncertainty to estimation of ground-water age. Furthermore, the age of discharging water after a pump is turned on would change in time as water from a larger and larger capture volume enters the well.

A hypothetical simulation illustrates use of the direct age method to model the time-evolution of age in water discharging from a pumping well in a highly heterogeneous formation. This simulation is based on a well-field scale model developed by Paul Hsieh (U.S. Geological Survey, written commun., 1994; see also Hsieh and Shapiro, 1996) of ground-water flow during an aquifer test in fractured rock at Mirror Lake, N.H. Shapiro and Hsieh (1996) provide an overview of research at the site on flow and transport in fractured rock. Aquifer hydraulic properties (table 1) were estimated by calibrating steady-state and transient models of three-dimensional flow during the test. These properties are used here in a model of steady-state age distribution and transient age transport during pumping tests.

The model grid is 22 rows *(y)* x 14 columns *(x)* x 38 layers *(z)*. The grid spacing is uniform throughout the grid with $\Delta x = \Delta y =$ 7.62 m, Δz = 1.5 m. The highly fractured zones of the bedrock are simulated as 1.5 m thick porous media units with much higher hydraulic conductivity than the surrounding bedrock (fig. 5).

Table 1. Hydraulic properties of a three-dimensional model of a highly heterogeneous formation (Paul A. Hsieh, U.S. Geological Survey, written commun., 1994).

		Hydraulic conductivity (meters per second)	
Hydrogeologic unit	Model layers	Horizontal	Vertical
Glacial drift	1-5	1.8×10^{-6}	1.8×10^{-6}
Bedrock surface	between 5 & 6	--	1.9×10^{-8}
Highly fractured	parts of 11, 22 & 38	5.6×10^{-5}	--
Less fractured	6-38	3.3×10^{-8}	1.9×10^{-7}

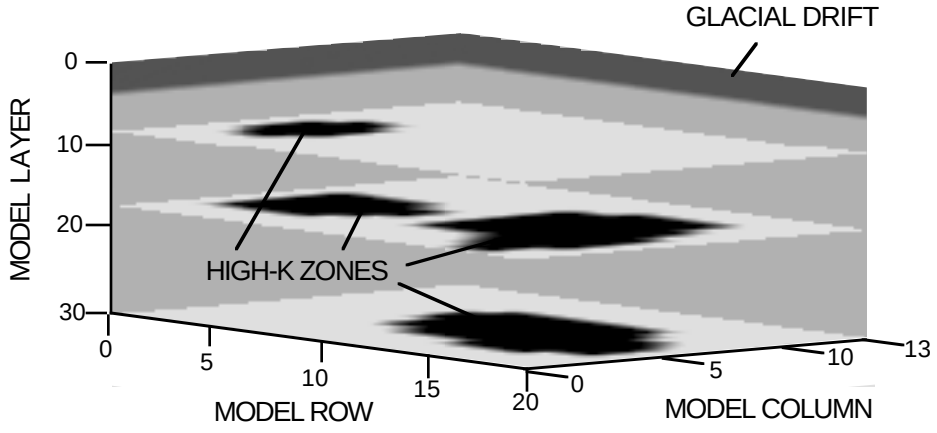

Figure 5. Horizontal hydraulic conductivity (*K*)distribution for three-dimensional highly-heterogeneous case. Glacial drift at top (dark gray) has $K = 1.8 \times 10^{-6}$ m/s (meters per second); four horizontal highly fractured zones (black) occur at three different depths and have $K = 5.6 \times 10^{-5}$ m/s; the remainder of the less-fractured bedrock has $K = 3.3 \times 10^{-8}$ m/s.

The initial steady-state distribution of ground-water age is assumed to represent conditions prior to pumping. The average annual recharge of 368 mm/yr (millimeters per year) is distributed over the top of the model. All other boundaries are no-flow, except the outflow face at y = 168 m, where the head in all model layers is fixed at 0.0. Age is simulated only in the bedrock part of the aquifer and it is assumed that all water inflowing from the glacial drift has age zero. For advection alone, the age distribution is efficiently computed by use of particle tracking. For the age simulation, the bedrock porosity is assumed to be 0.001, which corresponds to the fracture volume per unit volume of rock.

Maximum ages are at the bottom of the system, where less-fractured bedrock underlies the highly-fractured zones (figs. 6-8). Flow is generally downward from the glacial drift into the horizontal fracture zones and then laterally out along the outflow face (front face in fig. 6; right end of cross-section in fig 7). The fracture zone at the bottom of the model is shown as the area of light-gray near well 3 in fig. 6. The maximum ages are diluted downgradient from the dark-gray area beneath well 2 by much younger waters in the fracture flow system. Resulting outflow face ages are high only at the very bottom of the aquifer (fig. 8).

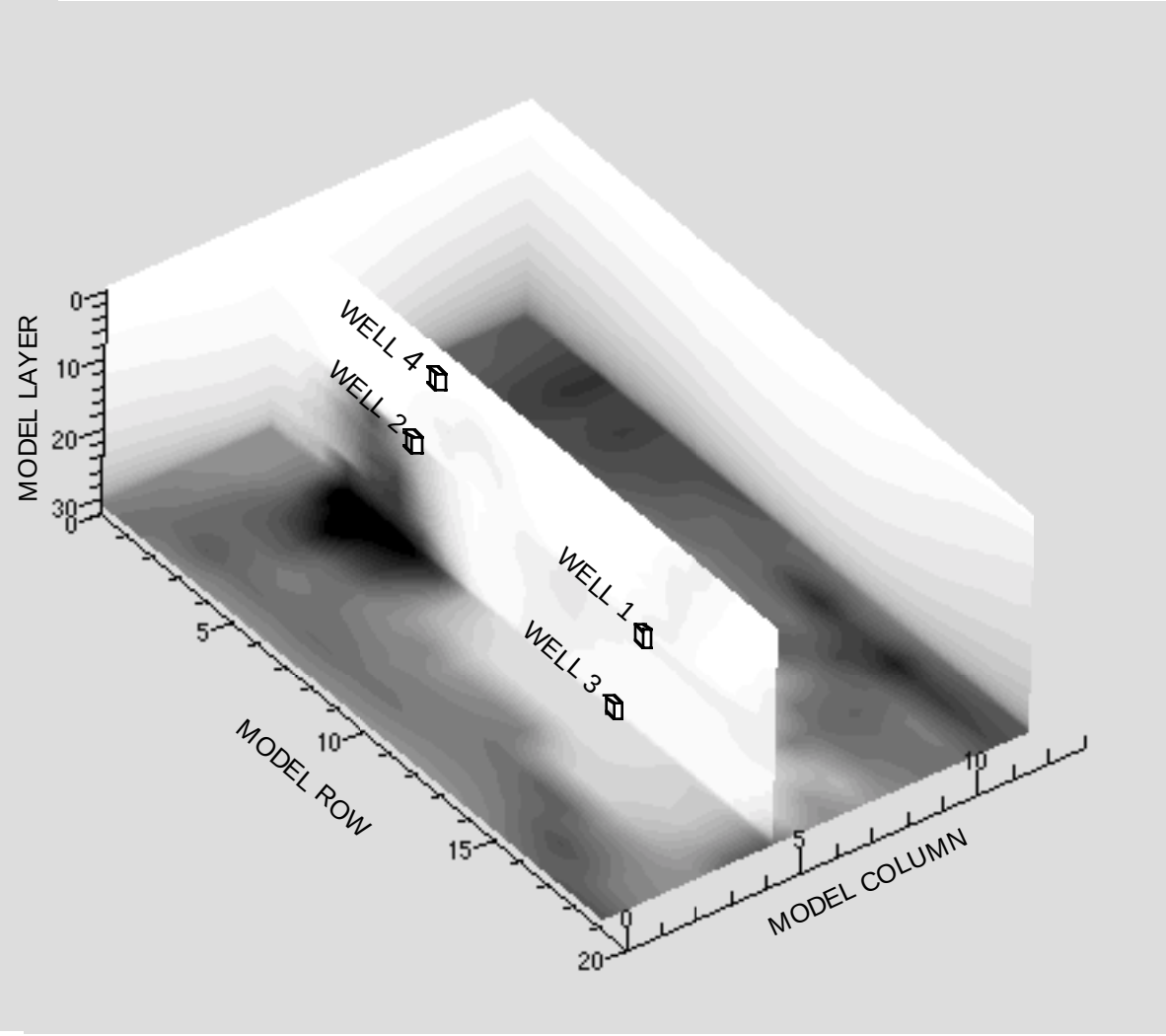

Figure 6. Results of direct simulation of steady-state ground-water age in a highly heterogeneous fractured bedrock. Hydraulic properties are shown in fig. 5 and summarized in table 1. Also shown are locations of wells that are not pumping in this simulation. The grayscale corresponds to age, ranging from less than 3 years (white) to greater than 700 years (black).

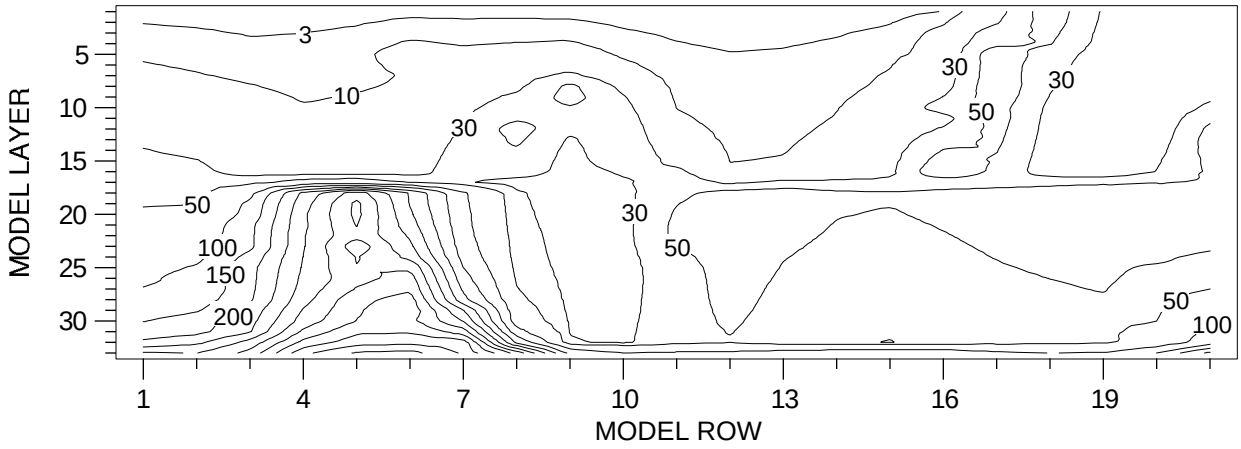

Figure 7. Results of direct simulation of steady-state ground-water age in a highly heterogeneous fractured bedrock in a *y-z* cross-section along the middle of the model at column 7 (x = 53 m), variable contour intervals in years.

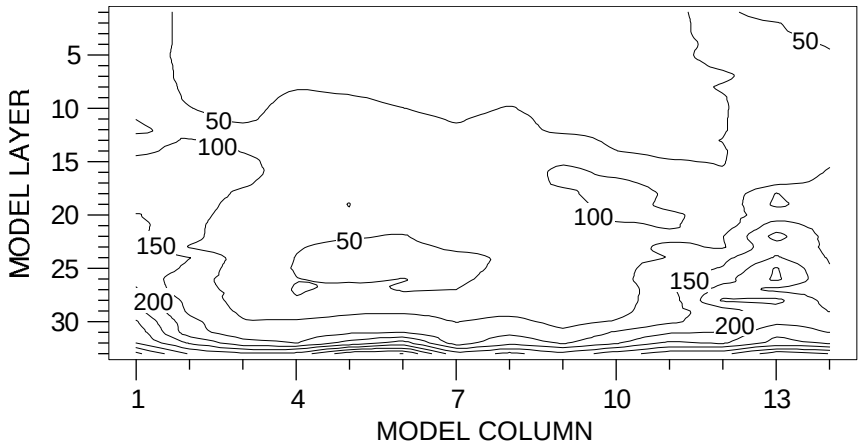

Figure 8. Results of direct simulation of steady-state ground-water age in a highly heterogeneous fractured bedrock in a *x-z* cross-section at the outflow end of the model along row 21 (y = 160 m), contour intervals are 50 years.

Ground-water age in pumped samples is evaluated for four fracture-zone well locations. In each case, the initial age distribution is that from the previous steady-state age simulation. A steady-state flow field is generated for each pumping scenario by imposing no-flow boundaries on the model bottom and all four sides. The top layer of the overburden is modeled as a fixed-head boundary from which all of the flow to the well is ultimately derived. Each well is pumped separately at a rate of 10.6 L/min (liters per minute).

The evolution of ground-water age of pumped samples is different for each well (fig. 9). Wells 1 and 2 are in upgradient fracture zones near mid-depth in the model. The age of water in well 1, which is closer to the outflow, increases sharply at early time from about 37 years to more than 40 years, levels off near 43 years, and appears to be gradually increasing after 10 hours of pumping. Well 2 pumps from a separate fracture zone at the same depth, and water from this well is initially older than that at well 1, even though it is farther from the outflow. The age of water in well 2 drops, but not as sharply in time, from 54 years to less than 46 years and then increases to about 56 years at the end of the simulation. The small-scale fluctuations in the age are numerical artifacts of the discrete method-of-characteristics model (Konikow and other, 1996).

Ground-water age in samples from wells 3 and 4 decrease logarithmically in time from the initial ages (fig. 9). Well 3 is located (fig. 5) in the bottom fracture zone and has the oldest initial age, over 200 years. However, the age decreases sharply to less than 120 years after 2 hours of pumping and is less than 100 years after 10 hours. Well 4 shows a similar pattern, but at much younger ages. This well is located in the top fracture zone, much closer

to the recharge source in the overburden. Ages in samples from well 4 decrease from more than 12.5 years initially to less than 8.5 years after 10 hours.

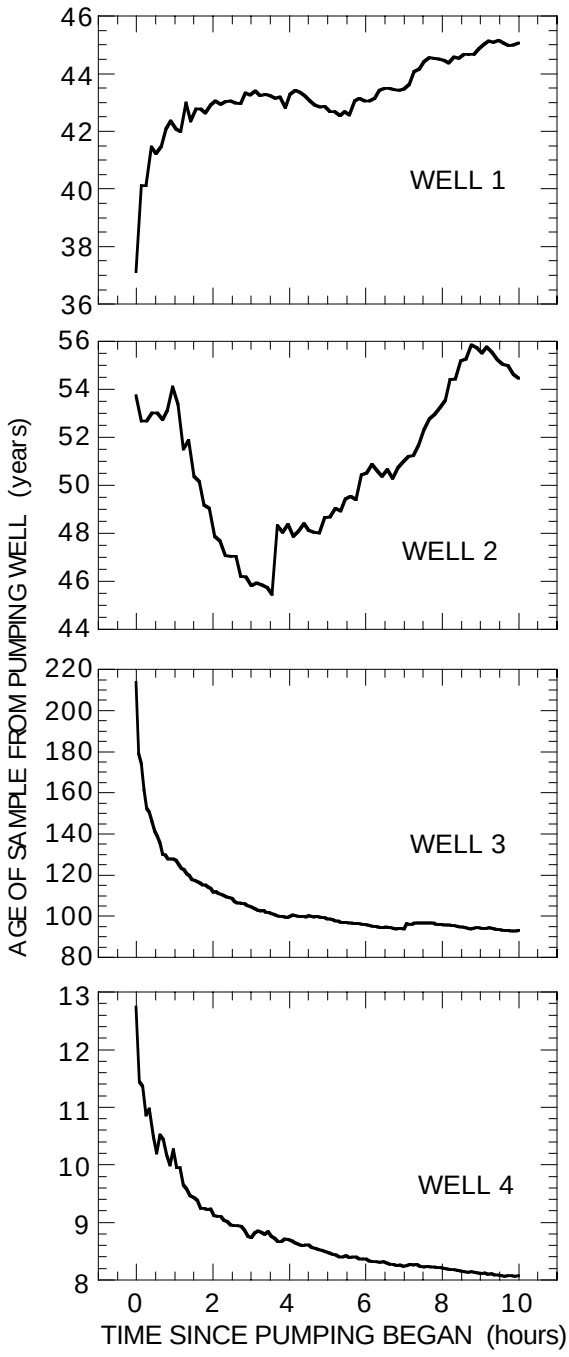

Figure 9. Sample age as a function of pumping time in a highly heterogeneous aquifer. Age transport to the pumping well is simulated with four different steady-state flow models having only the well of interest pumping. Locations for each well are shown in fig. 6.

Matrix Diffusion of Age in a Single Fracture

Matrix diffusion can be an important aspect of transport of solutes in ground water, particularly in fractured-rock settings (Shapiro, 1996). Matrix diffusion generally refers to diffusive exchange between high-permeability fractures or fracture zones and low-permeability rock matrix, whether much less fractured or unfractured. Water flow is primarily in the fractures, and the rock matrix is usually assumed to be impermeable. However, diffusive exchange of solutes between the flowing water in the fractures and the immobile water in the rock matrix can have significant effects on solute migration (Wood and others, 1996).

The age transport concept can be used to evaluate the effect of matrix diffusion on steady-state age distribution. Consider age transport in a fractured-rock system, which is modeled as advection and dispersion in a continuum of connected fractures, coupled with diffusion to and from the rock matrix. Normally, diffusion of water itself is ignored because the properties of individual water molecules are identical. In the case of age, however, diffusion of water changes the distribution of water ages. Under steady-state conditions, an integrated age conservation equation for the rock matrix has only three components: (1) accumulation of age (zero for steady state), (2) boundary flux, and (3) production of age by aging. Because (1) is zero in steady state, (2) and (3) must balance. Hence, the net boundary flux of age out of the rock matrix into the fracture is equal to the total age production rate in the matrix, which is the rock porosity. The rate of aging in the fracture and the added age flux from the rock matrix is equivalent to the aging rate of a single-porosity system in which the porosity is the sum of the fracture and rock matrix porosity.

Thus, the age distribution is identical to that of a single continuum system in which the porosity is the sum of the fracture and rock matrix porosities (Goode, 1998). The apparent velocity is ‘retarded’ compared to the velocity of water in the fractures alone, and the rate of dispersive spreading is likewise reduced by the total porosity. Of course, this analysis assumes that the age distribution is in steady state. Because of the slow rate of diffusion in rock, disequilibrium between the age production in the rock and diffusion out into the fracture may exist for millions of years.

The effect of matrix diffusion on transient age transport is examined here for a one-dimensional flow system using the double-porosity exchange process in MOC3D. A 1-m long column is discretized with 10 cells (Δx = 0.1 m). Imposed fixed-head boundary conditions yield a specific discharge of 1 m/d, and the porosity of 0.01 results in a uniform velocity of 100 m/d. This porosity represents the high-permeability fractures in the rock column. Ignoring dispersion and matrix diffusion, the steady-state age at x = 9.5 m is simply the advective traveltime, 0.095 day.

At steady state, the effect of matrix diffusion is an apparent increase in porosity, from that of the fractures alone to the sum of fracture and matrix porosity. In this case, the apparent traveltime to x = 9.5 m, and the steady-state age, is 0.95 day or an increase by an order-of-magnitude. This increase corresponds directly to the increase in porosity from 0.01 to 0.10. However, the rate at which this steady state is approached depends on the double-porosity exchange rate.

The linear exchange coefficient (β) is generally proportional to the diffusion coefficient (D_m) divided by a characteristic diffusion length (b) squared (Bibby, 1981):

$$\beta \propto \frac{D_m}{b^2} \quad . \qquad (1)$$

For example, for the case of planar fractures, the linear exchange coefficient corresponding to a one-node finite-difference approximation is given by:

$$\beta = \frac{1}{2}\frac{D_m}{b^2} \quad , \qquad (2)$$

where b is the block half-thickness. This simple linear model of matrix diffusion is strictly accurate only for relatively small diffusion distances. However, this kinetic exchange model can be considered a first-order approximation of the effect of exchange between high-permeability and much-lower-permeability portions of a flow system, whether limited strictly to diffusion or not.

The initial age is assumed to be zero throughout the aquifer. At early time, water at all locations ages as simulation time progresses (fig. 10). If the linear exchange coefficient is $\beta = 10^{-4}$ /day, the age temporarily stabilizes at a level corresponding to the traveltime in the fractures alone, 0.095 day (fig. 10). Eventually, however, the age in the matrix builds up to such high levels that the diffusive age flux into the fracture is sufficient to increase the age in the fractures and ultimately reach the steady-state value corresponding to the traveltime computed from the total porosity, 0.95 day. The magnitude of the linear exchange coefficient controls the time at which matrix diffusion has a significant effect on simulated ages in the fracture. For very high β, the initial plateau is not present because the fracture and matrix ages are virtually in equilibrium at all times (fig. 10).

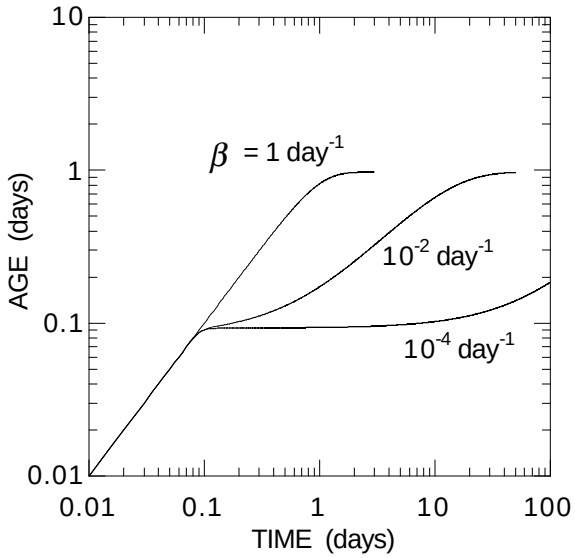

Figure 10. Age at x = 9.5 m from the inflow boundary of a one-dimensional rock column having fracture porosity 0.01, rock matrix porosity 0.09, and specific discharge 1 m/day. The initial condition is age = 0 at all locations. Age is shown as a function of simulation time for three values of linear exchange coefficient (β) characterizing the rate of mass transfer by diffusion between the flowing water in the fractures and the immobile water in the rock matrix.

SUMMARY

MOC3D can simulate transport of a single solute in saturated ground water under a wide range of conditions. New capabilities of the model include a zero-order internal source term that can vary in space and time; double-porosity exchange, which can approximate matrix diffusion and other rate-limited exchange processes; and simulation of ground-water age. Improved flexibility allows the retardation and first-order decay model components to more accurately approximate

biodegradation and other reactions that change in space and time due to changing geochemical conditions.

Example simulations demonstrate uses of MOC3D for transport simulation. These examples are drawn from research conducted at Laurel Bay, S.C., Cape Cod, Mass., and Mirror Lake, N.H., research sites under the U.S. Geological Survey Toxic Substances Hydrology Program. The spatially variable decay rate coefficients can be used to approximate biodegradation of organic contaminants in plumes having spatially variable biogeochemistry. The age transport model can account for mixing of waters of different ages caused by diffusion and dispersion, or by mixing in pumping wells. These new and extended capabilities improve the usefulness of MOC3D for simulation of solute transport in aquifers having variable hydraulic and geochemical conditions.

REFERENCES

Bibby, Robert, 1981, Mass transport of solutes in dual-porosity media: Water Resources Research, v. 17, no. 4, p. 1075-1081.

Garabedian, S.P., LeBlanc, D.R., Gelhar, L.W., and Celia, M.A., 1991, Large-scale natural gradient tracer test in sand and gravel, Cape Cod, Massachusetts 2. Analysis of spatial moments for a nonreactive tracer: Water Resources Research, v. 27, no. 5, p. 911-924.

Goode, D.J., 1996, Direct simulation of groundwater age: Water Resources Research, v. 32, no. 2, p. 289-296.

——— 1998, Ground-water age and atmospheric tracers: Simulation studies and analysis of field data from the Mirror Lake site, New Hampshire: Princeton, N.J., Princeton University, Dept. Civil Engineering and Operations Research, unpublished Ph.D. thesis, 194 p. <http://pa.water.usgs.gov/projects/frhr/thesis.html>

Harbaugh, A.W., and McDonald, M.G., 1996, User's documentation for MODFLOW-96, an update to the U.S. Geological Survey modular finite-difference ground-water flow model: U.S. Geological Survey Open-File Report 96-485, 56 p.

Hess, K.M., Wolf, S.H., and Celia, M.A., 1992, Large-scale natural gradient tracer test in sand and gravel, Cape Cod, Massachusetts 3. Hydraulic conductivity variability and calculated macrodispersivities: Water Resources Research, v. 28, no. 8, p. 2011-2027.

Hsieh, P.A., and Shapiro, A.M., 1996, Hydraulic characteristics of fractured bedrock underlying the FSE well field at the Mirror Lake site, Grafton County, New Hampshire, *in* Morganwalp, D.W. and Aronson, D.A., eds., U.S. Geological Survey Toxic Substances Hydrology Program—Proceedings of the technical meeting, Colorado Springs, Colo., September 20-24, 1993: U.S. Geological Survey Water-Resources Investigations Rep. 94-4015, p. 127-130.

Konikow, L.F., Goode, D.J., and Hornberger, G.Z., 1996, A three-dimensional method-of-characteristics solute-transport model (MOC3D): U.S. Geological Survey Water-Resources Investigations Report 96-4267, 87 p.

Landmeyer, J.E., Chapelle, F.H., Bradley, P.M., Pankow, J.F., Church, C.D., and Tratnyek, P.G., 1998, Fate of MTBE relative to benzene in a gasoline-contaminated aquifer (1993-98): Ground Water Monitoring and Remediation, v. 18, no. 4, p. 93-102.

LeBlanc, D.R., Garabedian, S.P., Hess, K.M., Gelhar, L.W., Quadri, R.D., Stollenwerk, K.G., and Wood, W.W., 1991, Large-scale natural gradient tracer test in sand and gravel, Cape Cod, Massachusetts 1. Experimental design and observed tracer movement: Water Resources Research, v. 27, no. 5, p. 895-910.

Mantoglou, A., and Wilson, J.L., 1982, The turning bands method for simulation of random fields using line generation by a spectral method: Water Resources Research, v. 18, no. 5, p. 1379-1394.

Plummer, L. N., Michel, R.L., Thurman, E.M. and Glynn, P.D., 1993,. Environmental tracers for age dating young ground water, *in* Alley, W.M., ed., *Regional Ground-Water Quality* , New York, Van Nostrand Reinhold, p. 255-294.

Shapiro, A.M., 1996, Using environmental tracers to estimate matrix diffusion in fractured rock over distances of kilometers: Results from the Mirror Lake site, New Hampshire [abs.]: Eos, Transactions American Geophysical Union, v. 77, no. 17, p. S107.

Shapiro, A. M., and Hsieh, P.A., 1996, Overview of research on use of hydrologic, geophysical, and geochemical methods to characterize flow and chemical transport in fractured rock at the Mirror Lake site, New Hampshire, *in* Morganwalp, D.W. and Aronson, D.A., eds., U.S. Geological Survey Toxic Substances Hydrology Program—Proceedings of the technical

meeting, Colorado Springs, Colo., September 20-24, 1993: U.S. Geological Survey Water-Resources Investigations Rep. 94-4015, p. 71-80.

Wood, W.W., Shapiro, A.M., Hsieh, P.A., and Councell, T.B., 1996, Observational experimental and inferred evidence for solute diffusion in fractured granite aquifers: Examples from Mirror Lake Watershed, Grafton County, New Hampshire, *in* Morganwalp, D.W. and Aronson, D.A., eds., U.S. Geological Survey Toxic Substances Hydrology Program—Proceedings of the technical meeting, Colorado Springs, Colo., September 20-24, 1993: U.S. Geological Survey Water-Resources Investigations Rep. 94-4015, p. 167-170.

Zimmerman, D.A., and Wilson, J.L., 1989, Description and user's manual for TUBA—A computer code for generating two-dimensional random fields via the turning bands method: Socorro, New Mexico Institute of Mining and Technology, unpublished report, Geosciences Department.

AUTHOR INFORMATION

Daniel J. Goode, U.S. Geological Survey, Malvern, Pennsylvania (djgoode@usgs.gov)